# Reaction of Horse Cytochrome *c* with the Radical and the Oxyferryl Heme in Cytochrome *c* Peroxidase Compound I†

Seung Hahm,‡ Mark A. Miller,§ Lois Geren,‡ Joseph Kraut,§ Bill Durham,‡ and Francis Millett*,‡

*Department of Chemistry and Biochemistry, University of Arkansas, Fayetteville, Arkansas 72701, and Department of Chemistry, University of California at San Diego, La Jolla, California 92093*

*Received July 16, 1993; Revised Manuscript Received November 15, 1993*®

ABSTRACT: The reactions of recombinant cytochrome *c* peroxidase [CcP(MI)] and a number of CcP(MI) mutants with native and ruthenium-labeled horse ferrocytochrome *c* have been studied by stopped-flow spectroscopy and laser flash photolysis. At 100 mM ionic strength, pH 7.5, native horse ferrocytochrome *c* reduces the radical on the indole group of Trp-191 in cytochrome *c* peroxidase compound I (CMPI) with a second-order rate constant of $1.3 \times 10^8$ $M^{-1}$ $s^{-1}$. Ferrocytochrome *c* then reduces the oxyferryl heme Fe(IV) in CMPII with a rate constant of $2.0 \times 10^6$ $M^{-1}$ $s^{-1}$. The rate constant for the reduction of the radical is nearly independent of pH from 5 to 8, but the rate constant for reduction of the oxyferryl heme Fe(IV) increases 33-fold as the pH is decreased from 8 to 5. This increase in rate is correlated with the pH dependence of the electron transfer equilibrium between the radical and the oxyferryl heme Fe(IV) in the transient form of CMPII. The second-order rate constants for reduction of the radical and the oxyferryl heme in the mutants Y39F, Y42F, H181G, W223F, and Y229F are nearly the same as for wild-type CcP(MI). The intracomplex rate constants for reduction of the radical in these mutants by the ruthenium-labeled cytochrome *c* derivatives are also similar to that for CcP(MI). This rules out a direct role for these aromatic residues in electron transfer. These results support reduction of both the radical at Trp-191 and the oxyferryl heme Fe(IV) by the pathway recently proposed by Pelletier and Kraut [(1992) *Science 258,* 1748–1755] on the basis of the crystal structure of the complex between yeast CcP(MI) and yeast iso-1-cytochrome *c*.

The cytochrome *c*–cytochrome *c* peroxidase system has been widely used for investigating fundamental questions about biological electron transfer. High-resolution crystallographic structures have been determined for both redox states of cytochrome *c* from a number of different organisms (Takano & Dickerson, 1981; Louie & Brayer, 1990). X-ray crystal structures have also been determined for yeast cytochrome *c* peroxidase in the resting, ferric state, CcP (Finzel et al., 1984), and the hydrogen peroxide oxidized state, CMPI (Edwards et al., 1987). In 1980, Poulos and Kraut proposed a hypothetical model for the 1:1 complex between tuna cytochrome *c* and cytochrome *c* peroxidase that was based on the crystal structures of the individual proteins. This model complex is stabilized by charge-pair interactions between lysines 13, 27, 72, 86, and 87 surrounding the heme crevice of cytochrome *c* and the carboxylate groups on Asp-34, -37, -79, and -216 on cytochrome *c* peroxidase. Very recently, Pelletier and Kraut (1992) determined the three-dimensional structure of a 1:1 complex between yeast cytochrome *c* peroxidase and yeast iso-1-cytochrome *c* crystallized at high ionic strength (150 mM NaCl, pH 7). The binding domain is different than that proposed in the Poulos–Kraut model, and hydrophobic and van der Waals interactions are particularly important in stabilizing the complex (Figure 1). No direct hydrogen bonds between the two proteins are present,

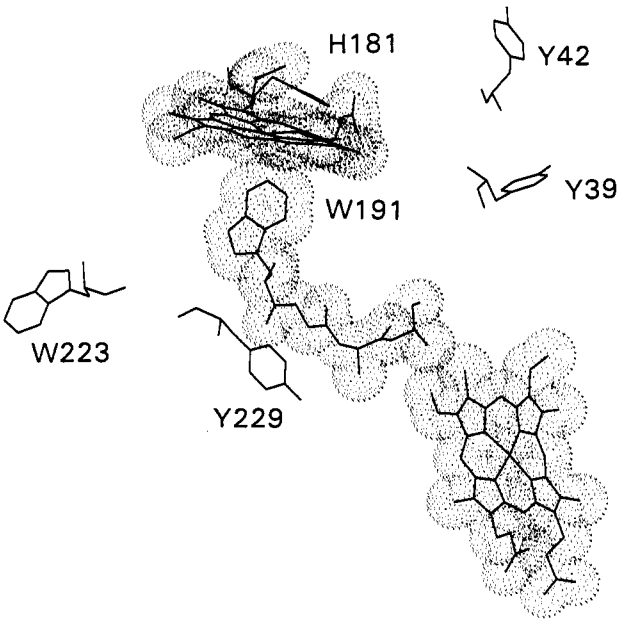


FIGURE 1: X-ray crystal structure of the complex between yeast cytochrome *c* peroxidase and yeast iso-1-cytochrome *c* (Pelletier & Kraut, 1992). The heme groups and the residues Trp-191, Gly-192, Ala-193, and Ala-194 proposed to be involved in the electron transfer pathway are enclosed in Connolly surfaces, and Tyr-39, Tyr-42, His-181, Trp-223, and Tyr-229 are labeled.

although the positive charges on cyt *c* lysines 73 and 87 are each about 4.2 Å from the negative charges on CcP Glu-290 and Asp-34, respectively. Thus, electrostatic interactions involving these residues as well as others stabilize the complex. Most importantly, the structure revealed a potential electron transfer pathway extending from the exposed heme methyl

† This work was supported in part by NIH Grant GM20488 (to F.M. and B.D.) and NSF Grant MCB 9119292 (to J.K. and M.M.).

* Author to whom correspondence should be addressed.
‡ University of Arkansas.
§ University of California at San Diego.

® Abstract published in *Advance ACS Abstracts,* January 15, 1994.

[1] Abbreviations: Ru-72-cyt *c*, bipyridine(4,4′-dicarboxybipyridine-Lys-72-cytochrome *c*) ruthenium(II).

0006-2960/94/0433-1473$04.50/0 

group CBC of cytochrome *c* through cytochrome *c* peroxidase residues Ala-194, Ala-193, and Gly-192 to the indole group of Trp-191, which is in van der Waals contact with the heme group.

In the mechanism for cytochrome *c* peroxidase, the resting ferric state, CcP, is oxidized by hydrogen peroxide to CMPI, which contains an oxyferryl heme Fe(IV) and a radical on the indole ring of Trp-191 (Mauro et al., 1988; Sivaraja et al., 1989; Erman et al., 1989; Fishel et al., 1991). CMPI is then sequentially reduced to CMPII and CcP in two one-electron reactions each involving ferrocytochrome *c* (Kim et al., 1990). Coulson et al. (1971) first reported two forms of the singly oxidized state, CMPII(IV,R) containing the oxyferryl heme Fe(IV), and CMPII(III,R•) containing the radical. They found that addition of 1 equiv of ferrocyanide or ferrocytochrome *c* to CMPI led to formation of CMPII(IV,R) at pH 7 and above but to formation of a mixture of CMPII(IV,R) and CMPII(III,R•) at pH 6 and below. On this basis they proposed the rapid equilibrium mechanism shown in Scheme 1.

Scheme 1

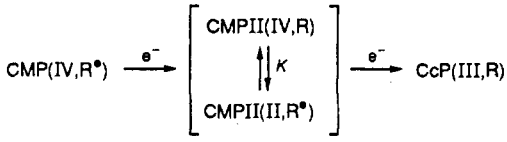


The horizontal arrows represent one-electron reduction of CMPI and CMPII, and the equilibration between the two forms of CMPII is assumed to be rapid compared to the reduction steps. The equilibrium constant $K$ is less than 0.13 at pH 7 and above but increases to 1.2 at pH 5 (Coulson et al., 1971). Ho et al. (1983, 1984) proposed that the rapid equilibrium between the two forms of CMPII only occurred in a transient intermediate, since CMPII(IV,R) formed by hydrogen peroxide oxidation of ferrous CcP was not converted to CMPII(III,R•) even at pH 5. It should be noted that CMPII(III,R•) has not been prepared or characterized in pure form, and there is only indirect evidence for its existence (Coulson et al., 1971; Ho et al., 1983, 1984).

A number of different rapid kinetics techniques have been used to study the reaction between cytochrome *c* and CMPI. Summers and Erman (1988) and Hazzard et al. (1987, 1988a–c, 1991) reported that cytochrome *c* initially reduced the heme Fe(IV) site in CMPI at low ionic strength using stopped-flow and flavin flash photolysis techniques, respectively. In contrast, Geren et al. (1991) and Hahm et al. (1992) found that five different ruthenium-labeled horse and yeast cytochrome *c* derivatives reacted first with the radical in CMPI and then with the Fe(IV) in CMPII at pH 7 according to Scheme 2:

Scheme 2

$$\text{CMPI(IV,R}^{\bullet}) + \text{cyt } c^{2+} \rightarrow \text{CMPII(IV,R)} + \text{cyt } c^{3+} \quad (1)$$

$$\text{CMPII(IV,R)} + \text{cyt } c^{2+} \rightarrow \text{CcP(III,R)} + \text{cyt } c^{3+} \quad (2)$$

This reaction mechanism was obeyed at both low and high ionic strength, and the rate constant for the intracomplex reaction with the radical at low ionic strength was very large (55 000 $s^{-1}$ for the cytochrome *c* derivative labeled at lysine 27). Hahm et al. (1993) have recently found that native horse cytochrome *c* also obeys this mechanism at high ionic strength and pH 7 and have developed a stopped-flow protocol to independently measure the second-order rate constants of reactions 1 and 2.

In the present paper we have studied the pH dependence of the reaction between horse cytochrome *c* and CMPI using stopped-flow spectroscopy. In addition, the potential role of aromatic residues in electron transfer was explored using the cytochrome *c* peroxidase mutants Y39F, Y42F, H181G, W191F, W223F, and Y229F. The reactions of cytochrome *c* with the radical and the Fe(IV) sites in each of these mutants were studied using both native horse cytochrome *c* and the ruthenium–cytochrome *c* derivatives over a wide range of ionic strength and pH conditions.

## EXPERIMENTAL PROCEDURES

*Materials.* Horse cytochrome *c* (type VI) was purchased from Sigma Chemical Co. Cytochrome *c* derivatives labeled at single lysine amino groups with (dicarboxybipyridine)-(bisbipyridine)ruthenium(II) (Ru-cyt *c*) were prepared as described by Pan et al. (1988) and Durham et al. (1989). CcP(MI) and mutants CcP(MI,Y39F), CcP(MI,Y42F), CcP-(MI,H181G), CcP(MI,W191F), CcP(MI,W223F), and CcP-(MI,Y229F) were prepared as described by Fishel et al. (1987, 1991) and Miller et al. (1988).

*Stopped-Flow Kinetics.* Transient kinetic studies were carried out on a Durrum model D-110 stopped-flow spectrophotometer equipped with a 2-cm flow cell as described by Hahm et al. (1993). The output was interfaced to a Biomation model 1010 waveform recorder and a PC for kinetic analysis. Ferricytochrome *c* was reduced with sodium ascorbate and the mixture was eluted on a 1 × 15 cm Bio-Gel P-2 column equilibrated with 2 mM sodium phosphate and 50 mM NaCl, pH 7.0, to remove ascorbate. One equivalent of $H_2O_2$ was added to CcP(MI), and the visible spectrum was recorded on a Hewlett-Packard HP 8452 spectrophotometer to confirm that CMPI was fully formed (Coulson et al., 1971). Ferrocytochrome *c* and CMPI in buffers containing sodium phosphate and NaCl (or potassium phosphate and potassium nitrate) were then placed in the two 2.5-mL syringes of the stopped-flow apparatus. All the transients were recorded within 1 min of CMPI formation at a series of different wavelengths. When the two syringes were nearly empty, the solutions were removed and visible spectra were recorded to verify that ferrocytochrome *c* and CMPI had remained stable.

The Durrum stopped-flow spectrophotometer placed certain constraints on the range of conditions that could be investigated. The instrument signal-to-noise ratio limited the minimum concentration of either reactant to about 0.3 μM, while the 2-ms dead time limited the maximum pseudo-first-order rate constant to 300 $s^{-1}$ for detection of at least 50% of the total absorbance change. For this reason, it was not possible in many cases to use a greater than 10-fold excess of one reactant in order to satisfy pseudo-first-order kinetics. Instead, the transients were fitted to the complete second-order equation

$$\Delta A = 2\Delta\epsilon\left(b_o - \frac{\exp[(b_o - a_o)kt] - 1}{\exp[(b_o - a_o)kt]/a_o - 1/b_o}\right) \quad (3)$$

where $b_o$ = initial [cyt $c^{2+}$], $a_o$ = [CMPI], and $\Delta\epsilon$ is the appropriate difference extinction coefficient. The difference extinction coefficients for oxidation of cytochrome *c* are $\Delta\epsilon_{416}$ = −40 $mM^{-1}$ $cm^{-1}$ and $\Delta\epsilon_{434}$ = 0 (Margoliash & Frohwirt, 1959). The following $\Delta\epsilon$ values for reduction of CMPI were estimated by interpolation of the graphical data of Coulson et al. (1971) and Ho et al. (1983): CMPI → CMPII(III,R•),

$\Delta\epsilon_{416} = -13$ mM$^{-1}$ cm$^{-1}$, $\Delta\epsilon_{434} = -27$ mM$^{-1}$ cm$^{-1}$; CMPI → CMPII(IV,R), $\Delta\epsilon < 3$ mM$^{-1}$ cm$^{-1}$ at both wavelengths.

The kinetics were studied using two different protocols. In protocol A, cyt $c^{2+}$ was mixed with excess CMPI at high enough ionic strength to ensure second-order kinetics. The second-order rate constant $k_a$ measured from the 416-nm transients represents all reactions involving oxidation of cyt $c^{2+}$ by CMPI. The typical range of concentrations was [cyt $c^{2+}$] = 0.3–1 $\mu$M and [CMPI] = 0.5–3 $\mu$M, always with [CMPI] > [cyt $c^{2+}$]. The second-order rate constants measured from the 416-nm transients using eq 3 were independent of concentration, confirming the second-order mechanism (Hahm et al., 1993). At pH 7 and higher essentially no absorbance change was detected at 434 nm, consistent with reduction of the radical rather than the oxyferryl heme Fe(IV) in CMPI. However, at lower pH values 434-nm transients were observed, indicating partial reduction of Fe(IV).

In protocol B excess cyt $c^{2+}$ was mixed with CMPI at high ionic strength. The second-order rate constant $k_b$ measured from the 434-nm transients represents all reactions involving reduction of the oxyferryl heme Fe(IV) by cyt $c^{2+}$. Typical concentrations were [cyt $c^{2+}$] = 1–10 $\mu$M and [CMPI] = 0.5 $\mu$M. The 434-nm transients were fitted to the full second-order eq 3. The 416- and 434-nm transients obtained with both protocols were also fitted to Schemes 3 and 4 using numerical integration methods (Strickland et al., 1975).

*Flash Photolysis Studies of Ru-Cyt c Derivatives.* Laser flash photolysis studies of the reactions between Ru-cyt *c* derivatives and cytochrome *c* peroxidase were carried out as described by Hahm et al. (1992). Ru-cyt *c* and cytochrome *c* peroxidase CMPI were prepared in 2 mM sodium phosphate, pH 6.4, 1–10 mM aniline, and 0–500 mM sodium chloride. Aniline was present to reduce Ru(III) to Ru(II) preventing the back-reaction. Aniline slowly reduces CMPI to CcP, so it was necessary to initiate flash photolysis within 1 min of CMPI formation. Under the conditions used, the reduction of CMPI by aniline was negligible, and the rate constants were independent of the concentration of aniline. The rate constants were also the same using EDTA as a sacrificial electron donor, which does not reduce CMPI (Hahm et al., 1992). The kinetic transients were fitted to a biexponential equation as described by Hahm et al. (1992).

## RESULTS

*Stopped-Flow Spectroscopy.* The reaction between native horse cytochrome *c* and recombinant CcP(MI) CMPI was studied using the stopped-flow protocols recently developed by Hahm et al. (1993). In protocol A, cyt $c^{2+}$ was mixed with an excess concentration of CMPI in order to measure the first electron transfer step in the reaction without possible complications arising from the second step. It was also found to be necessary to use high ionic strength in order to resolve the entire extent of the reaction in the stopped-flow instrument with a dead time of 2 ms. Figure 2 shows the reaction between 0.45 $\mu$M horse ferrocytochrome *c* and 0.48 $\mu$M CcP(MI) CMPI in 100 mM ionic strength buffer (4.2 mM potassium phosphate, pH 7.5, 90 mM $KNO_3$). The 416-nm transient indicated that all of the ferrocytochrome *c* was oxidized during the reaction. However, no absorbance change was observed at 434 nm, a cytochrome *c* isobestic. This indicates electron transfer from ferrocytochrome *c* to the radical in CMPI, since reduction of Fe(IV) would have been accompanied by a large decrease in absorbance at 434 nm. The wavelength dependence of the amplitude of the transient is the same as the $\Delta\epsilon$ for the oxidation of ferrocytochrome *c* (Hahm et al., 1993),

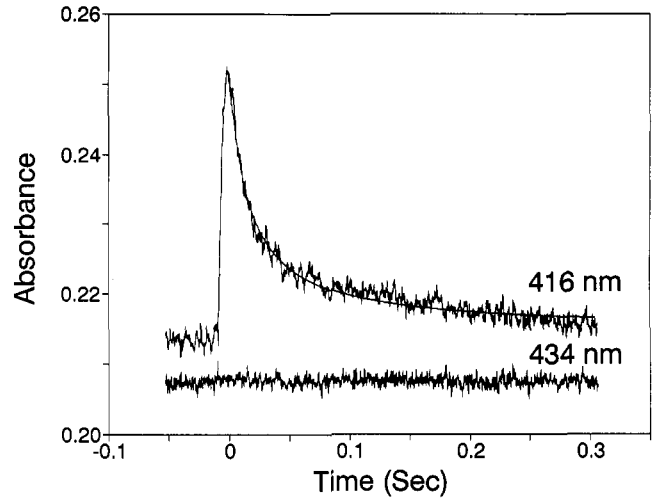


FIGURE 2: Stopped-flow reaction between horse ferrocytochrome *c* (0.45 $\mu$M) and CcP(MI) CMPI (0.48 $\mu$M) in 4.2 mM potassium phosphate, pH 7.5, and 90 mM $KNO_3$ at 25 °C. The reaction was monitored at 416 and 434 nm. The solid line is the best fit to the second-order eq 3 with $k = 1.3 \times 10^8$ M$^{-1}$ s$^{-1}$.

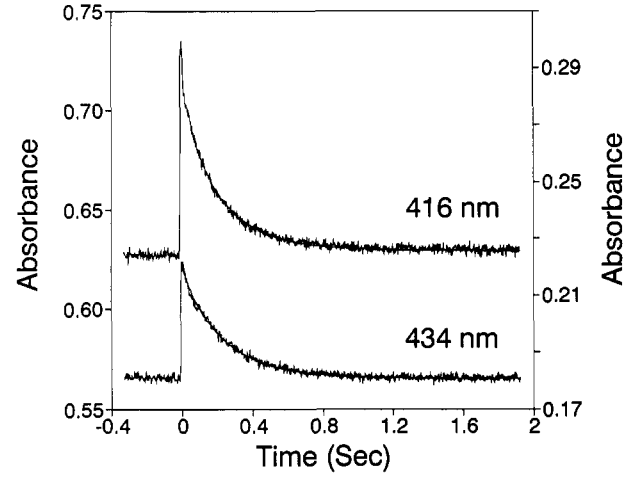


FIGURE 3: Stopped-flow reaction between ferrocytochrome *c* (3.0 $\mu$M) and CcP(MI) CMPI (0.6 $\mu$M) under the same conditions as Figure 2. The solid line in the 416-nm transient is the best fit of the slow phase to the second-order kinetic eq 3 with $k = 2.0 \times 10^6$ M$^{-1}$ s$^{-1}$. The solid line in the 434-nm transient is the best fit of the single phase to eq 3 with $k = 2.0 \times 10^6$ M$^{-1}$ s$^{-1}$. The 416-nm absorbance scale is on the left, and the 434-nm scale is on the right.

confirming electron transfer to the radical in CMPI. The $\Delta\epsilon$ for reduction of the radical is < 4 mM$^{-1}$ cm$^{-1}$ throughout the Soret region (Coulson et al., 1971). The reaction was confirmed to be second-order in experiments with CMPI concentrations ranging from 0.3 to 2 $\mu$M, with a rate constant of $k_a = (1.3 \pm 0.2) \times 10^8$ M$^{-1}$ s$^{-1}$.

In protocol B excess cyt $c^{2+}$ was mixed with CMPI in order to study complete reduction of CMPI to CcP. The 416-nm transient of the reaction between 3 $\mu$M cyt $c^{2+}$ and 0.5 $\mu$M CMPI was biphasic, while the 434-nm transient was monophasic (Figure 3). Both reactions of Scheme 2 are detected at 416 nm, while only reaction 2 is detected at 434 nm. The fast phase was only partially resolved with the stopped-flow time resolution and represented reaction 1 of Scheme 2. The slow phase of the 416-nm transient corresponded to the 434-nm transient and represented reaction 2. The second-order rate constant $k_b$ of reaction 2 was found to be $(2.0 \pm 0.2) \times 10^6$ M$^{-1}$ s$^{-1}$ in a series of experiments with the ferrocytochrome *c* concentration ranging from 1.5 to 10 $\mu$M.

The second-order rate constants $k_a$ and $k_b$ increased with decreasing ionic strength (Hahm et al., 1993). At ionic

Table 1: pH Dependence of the Rate Constants $k_a$ and $k_b$ in 8 mM Sodium Phosphate, with NaCl Added to a Total Ionic Strength of 10 mM[a]

| pH | $k_a$ | $k_b$ | $k_1$ | $K$ | $k_1'$ | $k_2'$ |
|---|---|---|---|---|---|---|
| 5.0 | 120 | 55 | 110 | 1.00 | 55 | 63 |
| 5.5 | 130 | 50 | 125 | 0.75 | 65 | 54 |
| 6.0 | 120 | 27 | 115 | 0.36 | 80 | 31 |
| 6.5 | 120 | 15 | 117 | 0.17 | 100 | 18 |
| 7.0 | 110 | 5.0 | 110 | 0.058 | 100 | 6.0 |
| 7.5 | 110 | 2.0 | 110 | 0.022 | 105 | 2.4 |
| 8.0 | 90 | 1.5 | 90 | 0.020 | 85 | 1.8 |

[a] The pH 5–6 buffers also contained 5 mM sodium acetate. $k_a$ was measured from 416-nm transients using excess CMPI (protocol A), while $k_b$ was measured from 434-nm transients using excess ferrocytochrome *c* (protocol B), both at 25 °C. The 416- and 434-nm transients were also fitted to Schemes 3 and 4 as described in the text, assuming that $k_2 = k_1$ in Scheme 3, and $k_3' = k_2'$ and $k_4' = k_1'$ in Scheme 4. The second-order rate constants are all given in units of $10^6$ $M^{-1}$ $s^{-1}$. The error in each parameter is ±20%.

strengths below 50 mM, $k_a$ exceeded $4 \times 10^8$ $M^{-1}$ $s^{-1}$, and less than 50% of the theoretical absorbance change was resolved in the 416-nm transient. At low ionic strength (4.2 mM potassium phosphate, pH 7.5), mixing 4.0 μM ferrocytochrome *c* with 4.2 μM CMPI resulted in a 416-nm transient with a rate constant of 300 ± 50 $s^{-1}$ and an absorbance change of 0.04 ± 0.01 AU, which corresponds to 12% of the theoretical value expected for complete oxidation of ferrocytochrome *c*. Almost no absorbance change was detected at 434 nm (<0.015 AU). Therefore, a substantial portion of the reaction was too fast to be resolved in the stopped-flow spectrophotometer. The rate constant $k_b$ measured at 434 nm using excess ferrocytochrome *c* also increases with decreasing ionic strength. However, more than 80% of the theoretical absorbance change for reduction of the oxyferryl heme Fe(IV) was resolved at 434 nm for all ionic strengths investigated (4–300 mM). The rate constant $k_b$ obtained by mixing 2.9 μM cyt $c^{2+}$ with 0.56 μM CMPI was 270 $s^{-1}$ in 2 mM sodium phosphate, pH 7.

The kinetics of the reactions shown in Scheme 1 were studied as a function of pH at a constant ionic strength of 110 mM. The second-order rate constant $k_a$ measured from the 416-nm transient using excess CMPI remained nearly constant at (1.2 ± 0.3) × $10^8$ $M^{-1}$ $s^{-1}$ from pH 5 to 8 (Table 1). No absorbance change was detected at 434 nm at pH 7. However, at lower pH a small 434-nm transient with decreasing absorbance was observed indicating partial reduction of Fe(IV). The rate constant of the 434-nm transient was the same as that of the 416-nm transient, indicating rapid equilibrium between the two forms of CMPII as shown in Scheme 1. At pH 5 the relative amplitudes of the 416- and 434-nm transients indicated that the equilibrium constant $K$ = CMPII(III,R•)/CMPII(IV,R) = 1.1 ± 0.3 after equilibrium was reached. The value of $K$ was 0.4 ± 0.2 at pH 6. At pH 8 a very small transient with increasing absorbance was observed at 434 nm with the same rate constant as the 416-nm transient. This transient is consistent with reduction of the radical in CMPI, since Coulson et al. (1971) reported a $\Delta\epsilon_{434}$ of 3 $mM^{-1}$ $cm^{-1}$ for this reaction. The absence of a 434-nm transient at pH 7 could, therefore, arise if an absorbance increase due to reduction of the radical is canceled by an equal absorbance decrease due to reduction of a very small fraction of the Fe(IV). However, the estimated $\Delta\epsilon_{434}$ for the radical is based on the subtraction of two spectra that are very similar in the Soret region, and the error in this extinction coefficient could be significant (Coulson et al., 1971). The equilibrium constant $K$ is therefore conservatively estimated to be ≤0.15 at pH 7 and ≤0.05 at pH 8.

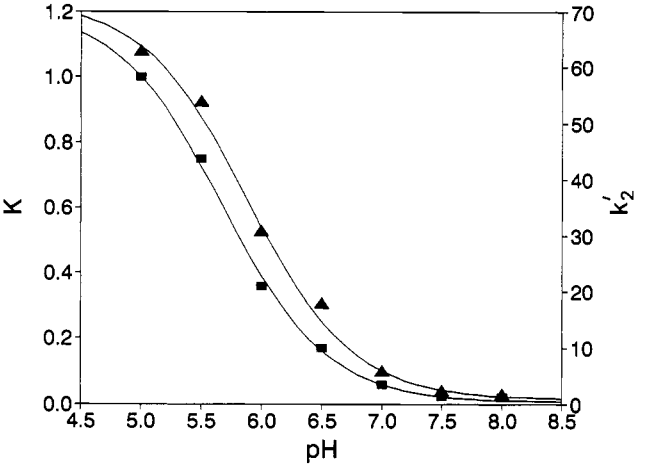


FIGURE 4: pH dependence of the reaction between ferrocytochrome *c* and CMPI in 8 mM sodium phosphate with NaCl added to a total ionic strength of 110 mM. (■) The values of $K$ for Scheme 3 obtained as described in Table 1 were fitted to the equation for a single ionization: $K = (K_l[H^+] + K_hK_a)/(K_a + [H^+])$, where $K_a$ is the acid dissociation constant, and $K_l$ and $K_h$ are the limiting values of $K$ at low and high pH, respectively. The best fit shown by the solid line was obtained with p$K_a$ = 5.7, $K_l$ = 1.21, and $K_h$ = 0.005. (▲) The values of $k_2'$ for Scheme 4 were fitted to the equation for a single ionization: $k_2' = (k_{2l}'[H^+] + k_{2h}'K_a)/(K_a + [H^+])$, where $k_{2l}'$ and $k_{2h}'$ are the limiting values of $k_2'$ at low and high pH, respectively. The best fit shown by the solid line was obtained with p$K_a$ = 5.9, $k_{2l}'$ = 7.2 × $10^7$ $M^{-1}$ $s^{-1}$, and $k_{2h}'$ = 8.0 × $10^5$ $M^{-1}$ $s^{-1}$. The units of $k_2'$ shown on the right axis of the figure are in $10^6$ $M^{-1}$ $s^{-1}$.

The second-order rate constant $k_b$ measured from the 434-nm transient using excess cyt $c^{2+}$ increased from 1.5 × $10^6$ to 5.0 × $10^7$ $M^{-1}$ $s^{-1}$ as the pH was decreased from 8.0 to 5.0 (Table 1). This apparent second-order rate constant represents all reactions resulting in reduction of the oxyferryl heme Fe(IV), either in CMPI or CMPII. Since Scheme 2 clearly is not applicable at low pH, a modified form of Scheme 1 was considered in which cytochrome *c* can react only with the radical in CMPI or CMPII(III,R•):

Scheme 3

$$\text{CMPI(IV,R}^\bullet\text{)} + \text{cyt } c^{2+} \xrightarrow{k_1} \text{CMPII(IV,R)} + \text{cyt } c^{3+}$$

$$\text{CMPII(IV,R)} \overset{K}{\rightleftarrows} \text{CMPII(III,R}^\bullet\text{)}$$

$$\text{CMPII(III,R}^\bullet\text{)} + \text{cyt } c^{2+} \xrightarrow{k_2} \text{CcP(III,R)} + \text{cyt } c^{3+}$$

Following reduction of the radical in CMPI(IV,R•), there is a rapid, pH-dependent equilibration of the transient form of CMPII(IV,R) with CMPII(III,R•), as suggested by Ho et al. (1983, 1984). This equilibration was assumed to be rapid compared to the reduction steps, consistent with the fact that the rate of the 434-nm transient is the same as that of the 416-nm transient at pH 5 under protocol A. In addition, the rate constant $k_2$ was assumed to be equal to $k_1$. The complete time courses for all the species in Scheme 3 were determined by numerical integration methods (Strickland et al., 1975). Both the 416- and 434-nm transients obtained with protocols A and B from pH 5 to 8 were accurately fit by Scheme 3 using the parameters shown in Table 1. The rate constant $k_1$ remained about the same at (1.2 ± 0.3) × $10^8$ $M^{-1}$ $s^{-1}$ from pH 5 to 8, while $K$ decreased from 1.0 to 0.02. The pH dependence of $K$ was fitted to single proton ionization with p$K_a$ = 5.7 ± 0.1, $K_{\text{low pH}}$ = 1.2, and $K_{\text{high pH}}$ = 0.005 (Figure 4).

Table 2: Second-Order Rate Constants $k_a$ and $k_b$ for Reactions between Horse Cytochrome c and CcP(MI) Mutants[a]

| mutant | $k_a$, pH 7 | $k_a$, pH 6 | $k_b$, pH 6 |
|---|---|---|---|
| CcP(MI) | 150 | 150 | 30 |
| Y39F | 140 | 160 | 34 |
| Y42F | 110 | 170 | 35 |
| H181G | | 100 | 24 |
| W223F | 150 | 160 | 40 |
| Y229F | 140 | 160 | 27 |

[a] $k_a$ and $k_b$ were measured as described in the text in 2 mM sodium phosphate, pH 6 or 7, and 100 mM NaCl. The second-order rate constants are given in units of $10^6$ $M^{-1}$ $s^{-1}$. The error limits are ±15%.

Coulson et al. (1971) also proposed an independent sites model for the reduction of CMPI by cyt $c^{2+}$, as shown in Scheme 4:

Scheme 4

$$\text{CMPI(IV,R}^\bullet\text{)} + \text{cyt } c^{2+} \xrightarrow{k_1'} \text{CMPII(IV,R)} + \text{cyt } c^{3+}$$

$$\text{CMPI(IV,R}^\bullet\text{)} + \text{cyt } c^{2+} \xrightarrow{k_2'} \text{CMPII(III,R}^\bullet\text{)} + \text{cyt } c^{3+}$$

$$\text{CMPII(IV,R)} + \text{cyt } c^{2+} \xrightarrow{k_3'} \text{CcP(III,R)} + \text{cyt } c^{3+}$$

$$\text{CMPII(III,R}^\bullet\text{)} + \text{cyt } c^{2+} \xrightarrow{k_4'} \text{CcP(III,R)} + \text{cyt } c^{3+}$$

Numerical integration techniques were used to fit Scheme 4 to the 416- and 434-nm transients obtained using protocols A and B. For simplicity, it was assumed that $k_3' = k_2'$ and $k_4' = k_1'$. Good fits were obtained over the pH range 5–8 using the rate constants given in Table 1. Small differences in the shapes of the transients simulated by Schemes 3 and 4 were observed, but the signal-to-noise ratio of the experimental transients was not sufficiently high to discriminate between the two schemes on this basis. The large pH dependence of $k_2'$ was fitted to a single proton ionization with $pK_a = 5.9 \pm 0.1$, $k_{21}' = 7.2 \times 10^7$ $M^{-1}$ $s^{-1}$, and $k_{2h}' = 8 \times 10^5$ $M^{-1}$ $s^{-1}$ (Figure 4).

The reactions between native horse cytochrome c and mutants of CcP(MI) were measured using protocol A at both pH 6 and 7 in 2 mM sodium phosphate and 100 mM NaCl. The $k_a$ rate constants of the mutants Y39F, Y42F, W223F, and Y229F were nearly the same as that of wild-type CcP(MI) at both pH values (Table 2). These mutants also displayed a small 434-nm transient under conditions of excess CMPI at pH 6, indicating partial reduction of Fe(IV). The ratio $K$ was 0.4 ± 0.2, the same as for wild-type CcP(MI). The $k_b$ rate constants for the reaction with the oxyferryl heme Fe(IV) in the mutants were measured at pH 6 in 2 mM sodium phosphate and 100 mM NaCl. The rate cosntants of Y39F, Y42F, W223F, and Y229F were essentially the same as that of CcP(MI), $(3.0 \pm 0.7) \times 10^7$ $M^{-1}$ $s^{-1}$ (Table 2). The CMPI form of the H181G mutant was stable at pH 6, but not at pH 7. The $k_a$ and $k_b$ rate constants for the H181G mutant at pH 6 were both somewhat smaller than that of CcP(MI) (Table 1).

*Flash Photolysis Studies with Ru-Cyt c Derivatives.* Intracomplex electron transfer between the Ru-cyt c derivatives and the radical in CcP(MI) mutants was studied at low ionic strength as described by Hahm et al. (1992). Photoexcitation of a sample containing 5 μM Ru-72 cyt c derivative and 6 μM CcP(MI) CMPI in 2 mM sodium phosphate, pH 6.4, and 10 mM aniline resulted in rapid reduction of the Ru-72-cyt c heme group followed by biphasic electron transfer

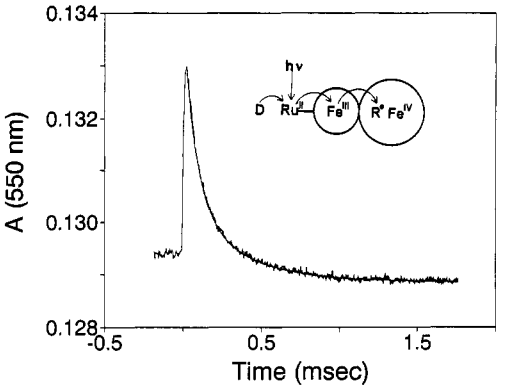


FIGURE 5: Photoinduced electron transfer between Ru-72 cyt c and CcP(MI) CMPI. The solution contained 5.0 μM Ru-72-cyt c and 6.0 μM CMPI(IV,R) in 2 mM sodium phosphate, pH 6.4, and 10 mM aniline. The 550-nm transient resulting from a single 450-nm laser flash was fit to the function $A[f\exp(-k_{etf}t) + (1-f)\exp(-k_{ets}t)]$ with $k_{etf}$ = 12 300 $s^{-1}$, $k_{ets}$ = 2200 $s^{-1}$, and $f$ = 0.67.

Table 3: Intracomplex Electron Transfer between Ru-cyt c Derivatives and the CMPI Form of CcP(MI) Mutants[a]

| | Ru-13-cyt c | | | Ru-27-cyt c | | | Ru-72-cyt c | | |
|---|---|---|---|---|---|---|---|---|---|
| Mutant | $k_f$ | $k_s$ | $f$ | $k_f$ | $k_s$ | $f$ | $k_f$ | $k_s$ | $f$ |
| CcP(MI) | 6.6 | 2.3 | 0.6 | 39 | 1.2 | 0.7 | 12 | 2.2 | 0.7 |
| Y39F | 6.0 | 1.7 | 0.6 | 46 | 1.5 | 0.6 | 16 | 1.4 | 0.5 |
| Y42F | 7.6 | 2.0 | 0.7 | 39 | 1.8 | 0.8 | 16 | 2.6 | 0.7 |
| H181G | 15.0 | 0.3 | 0.5 | 20 | 0.2 | 0.6 | 16 | 0.3 | 0.5 |
| W223F | | | | 40 | 0.6 | 0.6 | 15 | 1.5 | 0.6 |
| Y229F | 11.0 | 1.6 | 0.6 | 35 | 2.2 | 0.8 | 18 | 2.4 | 0.7 |

[a] The solutions contained 5 μM Ru-cyt c, 6–15 μM CMPI mutant in 2 mM sodium phosphate, pH 6.4, and 10 mM aniline at 25 °C. The rate constants were measured from biexponential fits of the 550-nm transients following a single laser flash as described in the legend Figure 5. The rate constants are in units of $10^3$ $s^{-1}$. $f$ is the fraction of the fast phase. The error limits are ±15%.

to CMPI (Figure 5). The fast phase had a rate constant of 12 500 $s^{-1}$ and a relative amplitude of 0.67, while the slow phase had a rate constant of 2200 $s^{-1}$ and a relative amplitude of 0.33. Both rate constants and relative amplitudes were independent of CMPI concentration as long as it was greater than the Ru-72-cyt c concentration, consistent with electron transfer within a 1:1 complex. Wavelength dependence studies in the Soret region verified that both phases involved electron transfer to the radical site in CMPI, as previously determined for the reaction with wild-type CcP at pH 7 (Hahm et al., 1992). The net decrease in absorbance at 550 nm is due to reduction of the radical (Hahm et al., 1992).

Reactions between Ru-cyt c derivatives and cytochrome c peroxidase mutants Y39F, Y42F, H181G, W223F, and Y229F also displayed biphasic kinetics at low ionic strength. The concentration independent rate constants are listed in Table 3. In most cases the fast phase rate constants of the Y39F, Y42F, W223F, and Y229F mutants were nearly the same as those of wild-type CcP(MI). There was somewhat greater variability in the rate constants of the slow phase. The greatest variability in rate constants was seen in the H181G mutant. The fast phase rate constant of H181G was more than 2-fold larger for Ru-13-cyt c and nearly 2-fold smaller for Ru-27-cyt c compared to CcP(MI). The slow phase rate constants were 8–10-fold smaller than those of CcP(MI). No transients were detected for solutions containing Ru-cyt c and the $H_2O_2$-oxidized W191F mutant, consistent with previous reports of very low reactivity of this mutant with cyt $c^{2+}$ (Mauro et al., 1988).

Ionic strength had a dramatic effect on the kinetics of the fast and slow phases of the reactions between the Ru-cyt *c* derivatives and the cytochrome *c* peroxidase mutants. As the ionic strength was increased from 2 mM sodium phosphate, pH 6.4, the fast phase rate constant and amplitude decreased and the slow phase rate constant and amplitude increased until a single phase was observed at 15–30 mM ionic strength, depending on the derivative. For the reaction between Ru-72-cyt *c* and CcP(MI), monophasic kinetics were observed at 20 mM ionic strength, and the rate constant displayed a hyperbolic dependence on CMPI concentration which was fit by

$$k_{obs} = k_{et}[C]/(K_d + [C]) \quad (4)$$

$k_{et}$ is the intracomplex rate constant from cyt *c* to CMPI, $K_d$ is a dissociation constant, and [C] is the concentration of CMPI. The best fit was obtained with $k_{et} = 6100\ s^{-1}$ and $K_d = 7\ \mu M$. The ionic strength dependencies of the Y39F, Y42F, W223F, and Y229F mutants were nearly the same as that of CcP(MI) (data not shown). The rate constants were somewhat smaller for the H181G mutant. For reaction between Ru-72 cyt *c* and H181G at 20 mM ionic strength, the monophasic rate constant had a hyperbolic dependence on peroxidase concentration, with $k_{et} = 3300\ s^{-1}$ and $K_d = 10\ \mu M$.

## DISCUSSION

*Mechanism of Reaction between Cytochrome c and CMPI.* The stopped-flow experiments at high ionic strength and pH of 7 or greater demonstrate that native horse ferrocytochrome *c* reacts first with the radical on Trp-191 of CcP(MI) CMPI according to reaction 1 of Scheme 2. A second molecule of ferrocytochrome *c* then reacts with the oxyferryl heme Fe(IV) in CMPII(IV,R) according to reaction 2. This mechanism is obeyed at pH values from 7 to 8, and ionic strengths from 50 mM to over 300 mM. The mechanism and rate constants are the same as for reaction with wild-type yeast CcP CMPI under the same ionic conditions (Hahm et al., 1993). Nuevo et al. (1993) also found that horse cytochrome *c* reduces CMPI according to Scheme 2 at ionic strengths above 100 mM, but at low ionic strength they reported that Fe(IV) was reduced initially. A number of other reductants preferentially reduce the radical in CMPI, including ferrocyanide (Jordi & Erman, 1974) and substituted anilines (Roe & Goodin, 1993). The present results suggest that horse cytochrome *c* might use the electron transfer pathway proposed by Pelletier and Kraut (1992) to reduce the radical on the indole group of Trp-191. The X-ray crystal structure determined for the complex between horse cytochrome *c* and cytochrome *c* peroxidase at low ionic strength is similar to the structure of the complex with yeast cytochrome *c* at high ionic strength (Pelletier & Kraut, 1992). The main differences are that the distance between the heme methyl group CBC on cytochrome *c* and the Ala-193, Ala-194 loop is much greater in the horse complex, 7 Å, and several charge-pair hydrogen bonds between the two proteins are present. Pelletier and Kraut (1992) suggested that at high ionic strength these charge-pair interactions might break, allowing horse cytochrome *c* to rotate slightly to an orientation allowing direct contact between the heme methyl group CBC and the Ala-193, Ala-194 loop. The proposed pathway from the cytochrome *c* heme methyl group CBC through cytochrome *c* peroxidase residues Ala-194, Ala-193, Gly-192, and Trp-191 provides a short, direct route for rapid electron transfer from ferrocytochrome *c* to the radical on the indole group of Trp-191.

An important question is whether the same binding site and reaction pathway are used for the reduction of the radical on Trp-191 and the oxyferryl heme Fe(IV). Insight into this question is provided by the pH dependence studies. At pH 8 no reduction of Fe(IV) is observed at 434 nm when ferrocytochrome *c* is mixed with excess CMPI using protocol A. However, at lower pH values partial reduction of Fe(IV) is observed in a 434-nm transient with the same rate constant as the 416-nm transient. The ratio $K$ = CMPII(III,R•)/CMPII(IV,R) obtained from the relative amplitudes of the 416- and 434-nm transients is $1.1 \pm 0.3$, $0.4 \pm 0.2$, $\leq 0.15$, and $\leq 0.05$ for pH values of 5, 6, 7, and 8, respectively. The pH dependence of this ratio is thus essentially the same as reported by Coulson et al. (1971) from equilibrium titration studies with ferrocytochrome *c* or ferrocyanide in 0.1 M potassium phosphate buffers. The rate constant $k_b$ for reduction of Fe(IV) measured from the 434-nm transient using protocol B increases 33-fold as the pH is decreased from 8 to 5 (Table 1). This dramatic pH dependence can be correlated with the pH dependence of the ratio $K$ obtained by Coulson et al. (1971) and in the present experiments using protocol A. This suggests that CMPII(IV,R) is first converted to CMPII(III,R•) before reduction by cyt $c^{2+}$ as assumed in Scheme 3. The entire pH dependence of the kinetics can be explained by Scheme 3 with an increase in $K$ from 0.02 to 1.0 as the pH is decreased from 8 to 5. The rate constants $k_1$ and $k_2$ for reduction of the radical in CMPI and CMPII(III,R•) remain nearly constant at $(1.2 \pm 0.3) \times 10^8\ M^{-1}\ s^{-1}$ throughout the pH range. The pH dependence of $K$ was well-fitted to a single ionization with $pK_a = 5.7 \pm 0.1$ (Figure 5). Thus it appears that the equilibrium between the radical and oxyferryl heme Fe(IV) could be controlled by a single ionizable residue in cytochrome *c* peroxidase.

An important consequence of Scheme 3 is that the same cytochrome *c* binding site and electron transfer pathway could be used for reduction of CMPI and CMPII. However, Scheme 3 is not a unique kinetic model for the stopped-flow data. The independent sites model (Scheme 4) proposed by Coulson et al. (1971) also provides a good fit to the kinetic data. In this scheme, the rate constant $k_1'$ for reduction of the radical in CMPI and CMPII(III,R•) was nearly independent of pH, while the rate constant $k_2'$ for reduction of Fe(IV) in CMPI and CMPII(IV,R) increased 35-fold as the pH was decreased from 8 to 5. A consequence of Scheme 4 is that the cytochrome *c* binding site and electron transfer pathway for reduction of the radical might be different from those for reduction of the oxyferryl heme Fe(IV). It was not possible to distinguish between Schemes 3 and 4 on the basis of the stopped-flow data alone. However, a number of other results support Scheme 3. First, it is supported by the fact that the ratio $K$ is the same using either ferrocyanide or ferrocytochrome *c* as reductant and also by kinetic studies of reduction by ferrocyanide (Coulson et al., 1971; Jordi & Erman, 1974). Second, the rate of reduction of Fe(IV) in the CcP(MI,W191F) mutant by horse cyt $c^{2+}$ is less than 0.1% that of wild-type CcP, even though the electronic properties of the oxyferryl heme Fe(IV) and the structure of this mutant appear to be similar to those of wild-type CMPI (Mauro et al., 1988; Wang et al., 1990). The Trp-191 indole group thus appears to be necessary for reduction of Fe(IV) by cyt $c^{2+}$. It should be noted that the steady-state peroxide-dependent oxidation of ferrocyanide by the W191F mutant is only 5–20-fold slower than that of CcP(MI) (Mauro et al., 1988). However, the very large concentration of ferrocyanide used in these experiments (8 mM) may have allowed multiple pathways for reduction. Third,

the second-order rate constants $k_a$ and $k_b$ have the same ionic strength dependence (Hahm et al., 1993). This indicates that the electrostatic interactions are similar for the two reactions, suggesting that the binding site for ferrocytochrome c could be the same.

Several other studies, however, suggest that Scheme 3 might not be complete at low ionic strength. The present studies indicate that, under conditions of excess CMPI, ferrocytochrome c reduces the radical site in CMPI with a rate that is too fast to be resolved in the stopped-flow at low ionic strength. However, Summers and Erman (1988) and Nuevo et al. (1993) reported that when excess ferrocytochrome c is mixed with CMPI at low ionic strength, the Fe(IV) site is initially reduced. This suggests that there might be a change in mechanism when ferrocytochrome c is present in excess, possibly due to multiple binding sites on cytochrome c peroxidase at low ionic strength. Hazzard et al. (1987) found that the stable form of CMPII(IV,R) prepared by the method of Ho et al. (1983) was reduced by ferrocytochrome c with an intracomplex rate constant of 450 $s^{-1}$ at low ionic strength and pH 7. Similarly, Hahm et al. (1992) measured an intracomplex rate constant of 350 $s^{-1}$ for the reaction between the stable form of CMPII(IV,R) and Ru-27-cyt c at pH 7. These rates are much faster than the rate of conversion of the stable form of CMPII(IV,R) to CMPII(III,R•) measured by Ho et al. (1984). Therefore, it appears that cytochrome c can directly reduce CMPII(IV,R) at low ionic strength in the absence of the radical.

*Potential Role of Aromatic Residues in Electron Transfer.* Prince and George (1990) proposed that a tyrosine side chain in CMPI might be transiently oxidized to a neutral radical by the Trp-191 radical or the oxyferryl heme Fe(IV), thus providing a pathway for electron transfer from cytochrome c. Tyr-39 is located on the surface of CcP within the Pelletier–Kraut binding domain, close to Leu-9 of cytochrome c (Figure 1). Tyr-39 is also located within the Poulos–Kraut binding domain (Poulos & Kraut, 1980). Tyr-42, another surface tyrosine, is located just outside the Pelletier–Kraut and Poulos–Kraut binding domains. Tyr-229 is the closest tyrosine to Trp-191 and is located on the surface just outside the Pelletier–Kraut binding domain (Figure 1). The proposal of Prince and George that one of these tyrosines could be transiently oxidized during electron transfer was tested by substitution with phenylalanine, which is much more difficult to oxidize. The second-order rate constants $k_a$ and $k_b$ for the mutants Y39F, Y42F, and Y229F are the same as for CcP(MI) (Table 2), indicating that these tyrosines do not play a direct role in electron transfer to either the radical on Trp-191 or the oxyferryl heme Fe(IV). Trp-223 is located on the surface close to the Poulos–Kraut binding domain and could potentially serve as an intermediate in electron transfer. This was ruled out by the finding that the W223F mutant has the same rate constants as CcP(MI) (Table 2). His-181 is located between the two heme groups in the Poulos–Kraut model and was postulated to provide a pathway for electron transfer (Poulos & Kraut, 1980). The rate constants of the H181G mutant are only slightly smaller than those of CcP(MI), confirming earlier kinetic studies showing that this residue is not essential for electron transfer (Miller et al., 1988).

The intracomplex electron transfer reactions between the Ru-cyt c derivatives and the CcP(MI) mutants were studied at low ionic strength by the laser flash photolysis technique (Hahm et al., 1992). Biphasic, concentration-independent reactions were observed between the Ru-cyt c derivatives and the radical in CMPI of each of the CcP(MI) mutants at low ionic strength (Table 3). The Ru-27-cyt c derivative is probably the most representative of native horse cytochrome c, since its second-order rate constant at high ionic strength is similar to that of native horse cytochrome c (Hahm et al., 1992). The kinetics of the Y39F, Y42F, and W223F mutants were nearly the same as that of CcP(MI), indicating that Tyr-39, Tyr-42, and Trp-223 are not involved in intracomplex electron transfer. The Y229F mutant had small differences in some of the fast-phase rate constants compared to Ccp-(MI), probably reflecting subtle changes in the conformation of the complex. The H181G mutant had the largest differences compared to CcP(MI), with a 2-fold decrease in the fast-phase rate constant for Ru-27-cyt c and a 2-fold increase for Ru-13-cyt c. These differences are probably due to changes in the conformation of the complex, rather than a direct role for His-181 in electron transfer. The slow phase rate constants of the H181G mutant were consistently 8–10-fold smaller than those of CcP(MI). The slow phase is believed to represent a fraction of the Ru-cyt c that is bound to an unreactive binding site on cytochrome c peroxidase. Oxidation of Ru-cyt c then requires dissociation from the unreactive site and binding to the reactive site (Hahm et al., 1992). The decreased slow phase rate constants for the H181G mutant thus probably reflects a decreased dissociation rate constant rather than a change in the electron transfer rate constant. It is tempting to speculate that this unreactive binding site is located at the original Poulos–Kraut binding site centered at His-181, and mutation of His-181 to Gly decreases the dissociation of cyt $c^{2+}$ from this site. As ionic strength is increased, the fast-phase rate constants decrease and the slow-phase rate constants increase until a single phase is observed at 20 mM ionic strength. This indicates rapid equilibration between the unreactive and reactive binding sites. The $k_{et}$ value for the reaction of Ru-72-cyt c with the H181G mutant is 3300 $s^{-1}$ at 20 mM ionic strength, only about 2-fold less than the value of 6100 $s^{-1}$ for CcP(MI). These results compare to $k_{et}$ values of 1850 and 3450 $s^{-1}$ for the reactions of native horse cyt $c^{2+}$ with H181G CMPI and CcP(MI) CMPI measured in 100 mM phosphate, pH 6, by a flavin flash photolysis technique (Miller et al., 1988). The decreased $k_{et}$ values for the H181G mutant at intermediate ionic strength could be due to preferential binding of cyt $c^{2+}$ to the unreactive binding site centered at His-181. The possibility that cytochrome c interacts with cytochrome c peroxidase at multiple binding sites has been investigated in a number of kinetics and binding studies (Mochan, 1970; Kang et al., 1977, 1978; Smith & Millett, 1980; Erman & Vitello, 1980; Kornblatt & English, 1986; Cheung & English, 1988; Hoffman & Ratner, 1987; Wallin et al., 1991; Everest et al., 1991; Vitello & Erman, 1987) as well as Brownian dynamics simulations (Northrup et al., 1987, 1988).

*Summary.* The reaction between horse cyt $c^{2+}$ and the radical on Trp-191 in CMPI is nearly independent of pH from pH 5 to 8 at 110 mM ionic strength, while the reaction with the oxyferryl heme Fe(IV) increases 33-fold as the pH decreases from 8 to 5. The kinetic results are consistent with either Scheme 3 or Scheme 4, but a number of other observations favor Scheme 3. The aromatic side chains on Tyr-39, Tyr-42, His-181, Trp-223, and Tyr-229 are not directly involved in electron transfer to either the radical or the oxyferryl heme Fe(IV). According to Scheme 3, cyt $c^{2+}$ can use the same binding site and electron transfer pathway to reduce both CMPI and CMPII. The electron transfer pathway proposed by Pelletier and Kraut (1992) on the basis of the crystal structure of the complex between CcP and yeast iso-

1-cyt *c* is consistent with these results.

## ACKNOWLEDGMENT

We thank Seong Park for excellent technical assistance and Rui-Qin Liu for performing several of the kinetic studies.

## REFERENCES

Coulson, A. J. W., Erman, J. E., & Yonetani, T. (1971) *J. Biol. Chem. 246*, 917–924.
Durham, B., Pan, L. P., Long, J., & Millett, F. (1989) *Biochemistry 28*, 8659–8665.
Cheung, E., & English, A. M. (1988) *Inorg. Chem. 27*, 1078–1081.
Edwards, S. L., Xuong, N. G., Hamlin, R. C., & Kraut, J. (1987) *Biochemistry 26*, 1503–1511.
Erman, J. E., & Vitello, L. B. (1980) *J. Biol. Chem. 255*, 6224–6227.
Erman, J. E., Vitello, L. B., Mauro, J. M., & Kraut, J. (1989) *Biochemistry 28*, 7992–7995.
Everest, A. M., Wallin, S. A., Stemp, E. D. A., Nocek, J. B., Mauk, A. G., & Hoffman, B. M. (1991) *J. Am. Chem. Soc. 113*, 4337–4338.
Finzel, B. C., Poulos, T. L., & Kraut, J. (1984) *J. Biol. Chem. 259*, 13027–13036.
Fishel, L. A., Villafranca, J. E., Mauro, J. B., & Kraut, J. (1987) *Biochemistry 26*, 351–360.
Fishel, L. A., Farum, M. F., Mauro, J. M., Miller, M. A., Kraut, J., Liu, Y., Tan, X., & Scholes, C. P. (1991) *Biochemistry 30*, 1986–1996.
Geren, L. M., Hahm, S., Durham, B., & Millett, F. (1991) *Biochemistry 30*, 9450–9457.
Hahm, S., Durham, B., & Millett, F. (1992) *Biochemistry 31*, 3472–3477.
Hahm, S., Geren, L., Durham, B., & Millett, F. (1993) *J. Am. Chem. Soc. 115*, 3372–3373.
Hazzard, J. T., & Tollin, G. (1991) *J. Am. Chem. Soc. 113*, 8956–8957.
Hazzard, J. T., Poulos, T., & Tollin, G. (1987) *Biochemistry 26*, 2836–2848.
Hazzard, J. T., McLendon, G., Cusanovich, M. A., & Tollin, G. (1988a) *Biochem. Biophys. Res. Commun. 151*, 429–434.
Hazzard, J. T., Moench, S. J., Erman, J. E., Satterlee, J. D., & Tollin, G. (1988b) *Biochemistry 27*, 2002–2008.
Hazzard, J. T., Mclendon, G., Cusanovich, M. A., Das, G., Sherman, F., & Tollin, G. (1988c) *Biochemistry 27*, 4445–4451.
Ho, P. S., Hoffman, B. M., Kang, C. H., & Margoliash, E. (1983) *J. Biol. Chem. 258*, 4356–4363.
Ho, P. S., Hoffman, B. M., Solomon, N., Kang, C. H., & Margoliash, E. (1984) *Biochemistry 23*, 4122–4128.
Hoffman, B. M., & Ratner, M. A. (1987) *J. Am. Chem. Soc. 109*, 6237–6243.
Jordi, H. C., & Erman, J. E. (1974) *Biochemistry 13*, 3734–3745.
Kang, C. H., Ferguson-Miller, S., & Margoliash, E. (1977) *J. Biol. Chem. 252*, 919–926.
Kang, C. H., Brautigan, D. L., Osheroff, N., & Margoliash, E. (1978) *J. Biol. Chem. 253*, 6502–6510.
Kim, K. L., Kang, D. S., Vitello, L. B., & Erman, J. E. (1990) *Biochemistry 29*, 9150–9159.
Kornblatt, J. A., & English, A. M. (1986) *Eur. J. Biochem. 155*, 505–511.
Louie, G. V., & Brayer, G. D. (1990) *J. Mol. Biol. 214*, 527.
Margoliash, E, & Frowirt, N. (1959) *Biochem. J. 71*, 570–575.
Mauro, J. M., Fishel, L. A., Hazzard, J. T., Meyer, T. E., Tollin, G., Cusanovich, M. A., & Kraut, J. (1988) *Biochemistry 27*, 6243–6256.
Miller, M. A., Hazzard, J. T., Mauro, J. M., Edwards, S. L., Simons, P. C., Tollin, G., & Kraut, J. (1988) *Biochemistry 27*, 9081–9088.
Mochan, E. (1970) *Biochim. Biophys. Acta 216*, 80–95.
Northrup, S. H., Boles, J. O., & Reynolds, J. C. L. (1987) *J. Phys. Chem. 91*, 5991–5998.
Northrup, S. H., Boles, J. O., & Reynolds, J. C. L. (1988) *Science 241*, 67–70.
Nuevo, M. R., Chu, H.-H., Vitello, L. B., & Erman, J. E. (1993) *J. Am. Chem. Soc. 115*, 5873–5874.
Pan, L. P., Durham, B., Wolinska, J., & Millett, F. (1988) *Biochemistry 27*, 7180–7184.
Pelletier, H., & Kraut, J. (1992) *Science 258*, 1748–1755.
Poulos, T. L., & Kraut, J. (1980) *J. Biol. Chem. 255*, 10322–10330.
Prince, R. C., & George, G. N. (1990) *Trends Biochem. Sci. 15*, 170–172.
Roe, J. A., & Goodin, D. B. (1993) *J. Biol. Chem. 268*, 20037–20045.
Sivaraja, M., Goodin, D. B., Smith, M., & Hoffman, B. M. (1989) *Science 245*, 738–740.
Smith, M. B., & Millett, F. (1980) *Biochim. Biophys. Acta 626*, 64–72.
Strickland, S., Palmer, G., & Massey, B. (1975) *J. Biol. Chem. 250*, 4048–4052.
Summers, F. E., & Erman, J. E. (1988) *J. Biol. Chem. 263*, 14267–14275.
Takano, T., & Dickerson, R. E. (1981) *J. Mol. Biol. 153*, 79.
Vitello, L. B., & Erman, J. E. (1987) *Arch. Biochem. Biophys. 258*, 621–629.
Wallin, S. A., Stemp, E. D. A., Everest, A. M., Nocek, J. M., Netzel, T. L., & Hoffman, B. M. (1991) *J. Am. Chem. Soc. 113*, 1842–1844.
Wang, J., Mauro, J. M., Edwards, S. L., Oatley, S. J., Fishel, L. A., Ashford, V. A., Xuong, N. H., & Kraut, J. (1990) *Biochemistry 29*, 7160–7173.